Coordination Complexes of Decamethylytterbocene with 4,4′-Disubstituted Bipyridines: An Experimental Study of Spin Coupling in Lanthanide Complexes

Marc D. Walter, David J. Berg, and Richard A. Andersen*

Department of Chemistry and Chemical Sciences Division of Lawrence Berkeley National Laboratory, University of California, Berkeley, California 94720

Received December 8, 2005

The paramagnetic 1:1 coordination complexes of $(C_5Me_5)_2Yb$ with a series of 4,4′-disubstituted bipyridines, bipy−X, where X is Me, *t*-Bu, OMe, Ph, CO_2Me, and CO_2Et, have been prepared. All of the complexes are paramagnetic, and the values of the magnetic susceptibility as a function of temperature show that these values are less than expected for the cations, $[(C_5Me_5)_2Yb(III)(bipy\text{-}X)]^+$, which have been isolated as the cation−anion ion pairs $[(C_5Me_5)_2Yb(III)(bipy\text{-}X)]^+[(C_5Me_5)_2YbI_2]^-$, where X is CO_2-Et, OMe, and Me. The ^1H NMR chemical shifts (293 K) for the methine resonances located at the 6,6′ site in the bipy−X ring show a linear relationship with the values of χT (300 K) for the neutral complexes, which illustrates that the molecular behavior does not depend on the phase, with one exception, viz., $(C_5Me_5)_2Yb$(bipy-Me). Single crystals of the 4,4′-dimethylbipyridine complex undergo an irreversible, abrupt first-order phase change at 228 K that shatters the single crystals. The magnetic susceptibility, represented in a χ vs T plot, on this complex, in polycrystalline form undergoes reversible abrupt changes in the temperature regime 205−212 K, which is suggested to be due to the way the individual molecular units pack in the unit cell. A qualitative model is proposed that accounts for the subnormal magnetic moments in these ytterbocene−bipyridine complexes.

Introduction

The preparation and the molecular and electronic structure of the coordination complexes of cyclopentadienyl-ring-substituted ytterbocenes with bipyridine of the type Cp'_2Yb(bipy), where Cp′ is C_5H_5, 1,3-$R_2C_5H_3$ (R = Me_3C, Me_3Si), 1,2,4-$R_3C_5H_2$ (R = Me_3C, Me_3Si), C_5Me_4H, or C_5Me_5 (Cp*), have been described.[1,2] Magnetic susceptibility measurements, as a function of temperature, of these simple coordination complexes and therefore their electronic structure are not simple to understand. The ytterbocene complexes are paramagnetic, which is unexpected since their stoichiometry implies they are based upon Yb(II) with a closed shell $4f^{14}$ electron configuration. Their paramagnetic condition implies that their electronic structure is based upon Yb(III) with an open shell electron configuration of $4f^{13}$, which requires that the bipyridine ligand carries a negative charge and is therefore noninnocent. However, the values of μ_{eff} as a function of temperature are much less than expected for the valence bond structure, [Cp′Yb(III, $4f^{13}$)][bipy$^{\bullet-}$, $S = {}^1/_2$], in which the charge carriers are uncoupled. Two ways that μ_{eff} can be lowered are either an equilibrium between the two valence bond structures [Yb(III), $4f^{13}$)][bipy$^{\bullet-}$, $S = {}^1/_2$] and [Yb(II), $4f^{14}$)][bipy, $S = 0$] or electron exchange coupling between the spin carriers in the paramagnetic spin isomer. The equilibrium model is appealing since the relative population of the two valence bond structures will determine the value of μ_{eff}, which in turn depends on the temperature, resulting in a temperature dependence of μ_{eff}. However, it has been shown recently for $(C_5Me_5)_2Yb$(bipy) that the Yb L_{III} edge XANES signatures for the Yb(II) and Yb(III) species do not change over the temperature regime 10−400 K, which is inconsistent with an equilibrium model.[3] The electron exchange coupling model is difficult to accept since the conventional view is that electrons in f-orbitals are core electrons that do not participate to any extent in chemical bonding in molecular compounds, and therefore the bonds between lanthanide metals and their ligands are largely due to electrostatic forces described by Coulomb's law. The exchange coupling model defines the parameter J, which is the coupling constant

* To whom correspondence should be addressed. E-mail: raandersen@lbl.gov.

(1) Schultz, M.; Boncella, J. M.; Berg, D. J.; Tilley, T. D.; Andersen, R. A. *Organometallics* **2002**, *21*, 460−472.

(2) Walter, M. D.; Schultz, M.; Andersen, R. A. *New J. Chem.* **2006**, *30*, 238−246.

(3) Booth, C. H.; Walter, M. D.; Daniel, M.; Lukens, W. W.; Andersen, R. A. *Phys. Rev. Lett.* **2005**, *95*, 267202.

(4) van Vleck, J. H. *The Theory of Electric and Magnetic Susceptibilities*; Clarendon Press: Oxford, 1932.

(5) Berg, D. J.; Boncella, J. M.; Andersen, R. A. *Organometallics* **2002**, *21*, 4622−4631.

(6) Ohsawa, Y.; Whangbo, M.-H.; Hanck, K. W.; DeArmond, M. K. *Inorg. Chem.* **1984**, *23*, 3426−3428.

(7) McInnes, E. J. L.; Farley, R. D.; Rowlands, C. C.; Welch, A. J.; Rovatti, L.; Yellowlees, L. J. *J. Chem. Soc., Dalton Trans.* **1999**, 4203−4208.

(8) Hansch, C.; Leo, A.; Taft, R. W. *Chem. Rev.* **1991**, *91*, 185−195.

(9) Finke, R. G.; Keenan, S. R.; Schiraldi, D. A.; Watson, P. L. *Organometallics* **1986**, *5*, 598−601.

(10) Da Re, R. E.; Kuehl, C. J.; Brown, M. G.; Rocha, R. C.; Bauer, E. D.; John, K. D.; Morris, D. E.; Shreve, A. P.; Sarrao, J. L. *Inorg. Chem.* **2003**, *42*, 5551−5559.

(11) Tilley, T. D.; Boncella, J. M.; Berg, D. J.; Burns, C. J.; Andersen, R. A. *Inorg. Synth.* **1990**, *27*, 146−149.

(12) We mentioned in ref 1 that the magnetic susceptibility of Cp^*_2Yb(bipy-Me) is superimposable on that of Cp^*_2Yb(bipy-H). We observed the discontinuity in its magnetic susceptibility vs temperature plot, but at that time we attributed this to temperature instability in the SQUID magnetometer that was used. This rationalization is no longer acceptable.

(13) Cotton, F. A.; Wilkinson, G. *Advanced Inorganic Chemistry*, 6th ed.; John Wiley & Sons: New York, 1988.

(14) Pauling, L. *The Nature of the Chemical Bond*; Cornell University Press: Ithaca, NY, 1960.

10.1021/om051051d CCC: $33.50
Publication on Web 05/19/2006

Table 1. Redox Potentials of 4,4′-X_2-bipy (bipy−X) in 0.1 M [^{n}Bu$_4$N][BF$_4$]−DMF at 293 K[6,7]

X	E_1[a]/V	E_2/V
OEt	−2.88[b]	
Me	−2.68[c] (0.140)[d]	
H	−2.60 (0.100)	
Ph	−2.34 (0.060)	
Cl	−2.24[b]	
CO_2Et	−2.05[e]	−2.40[e]
CO_2Me	−2.03 (0.070)	−2.52 (0.130)

[a] Potentials quoted relative to $[Cp_2Fe]^+/Cp_2Fe$, measured relative to Ag−AgCl. [b] Irreversible, cathodic peak quoted. [c] $(E_f - E_r)/2$. [d] $E_f - E_r$. [e] 0.1 M $[Et_4N][PF_6]$−DMF at −54 °C.[6]

or exchange integral in the Schroedinger Heisenberg Van Vleck Hamiltonian, $\hat{H} = J\vec{S}_1 \cdot \vec{S}_2$,[3,4] and the value of J must be large (>500 cm^{-1}) and negative (antiferromagnetic coupling) in order to account for the low values of μ_{eff} observed.[1,2] Qualitatively, the large value of the exchange interaction means that the unpaired electron in the f-orbital of the Cp*$_2$Yb(III) fragment and the electron in the ligand LUMO of the bipy$^{\bullet-}$ are strongly coupled; that is, they are participating in a bonding interaction. In the electrostatic bonding model, exchange interaction is introduced by polarization, but these values are small, on the order of 10−25 cm^{-1}.[5] Thus the ytterbocene−bipy compounds provide fertile ground for exploring bond models that provide a deeper understanding of the electronic structure of f-block metal compounds in general and the metallocenes in particular.

The original papers focused on a series of ytterbocene−bipy coordination compounds in which the substituents on the cyclopentadienyl ring changed the magnetic properties of the resulting complexes.[1,2] In this paper the focus is on how the magnetic susceptibility changes when the cyclopentadienyl ring is kept constant, in this case C_5Me_5, and the substituents on the 4,4′-position of bipyridine are changed. Therefore, the role of substituents in tuning the magnetic properties of the coordination compounds can be experimentally defined, a prerequisite for developing a bond model.

Results and Discussion

Synthesis. The most readily available substituted bipyridine derivatives are those substituted in the 4,4′-position (the position *para* to the nitrogen atom in the ring). The steric bulk of the substituents at these remote sites should have an insignificant influence on intramolecular steric effects, but the electronic effects will change significantly. This is supported by the reduction potentials of the free ligand, shown in Table 1.

These values show that the substituents used in this study alter the redox potentials by 0.85 V as the substituent changes from OEt (and by assumption OMe, used in this work), an electron-donating group, to CO_2Me, an electron-withdrawing group. This substituent effect is consistent with the Hammett σ-constants.[8] The uncoordinated bipyridine ligands used in this work cannot be reduced by $(C_5Me_5)_2Yb$, since its reduction potential in acetonitrile is +1.78 V relative to Cp_2Fe/Cp_2Fe^+.[9] Presumably the reduction potential of the free ligand is lowered when it binds to the Lewis acid.[10]

The substituted bipyridine adducts of decamethylytterbocene are prepared by adding the bipyridine ligand (bipy−X) to a solution of $(C_5Me_5)_2Yb(OEt_2)$, Cp*$_2$Yb(OEt$_2$), in toluene and crystallizing the red complexes from toluene or pentane, eq 1. Some physical properties of the complexes are listed Table 2.

$$Cp^*_2Yb(OEt_2) + 4,4'\text{-}X_2\text{-bipy} \rightarrow Cp^*_2Yb(4,4'\text{-}X_2\text{-bipy}) + OEt_2$$

$$X = CO_2Me,\ CO_2Et,\ Ph,\ H,\ Me,\ t\text{-}Bu,\ OMe \qquad (1)$$

These complexes are high-melting solids, when they melt, but do not sublime when heated in diffusion pump vacuum; they decompose at temperatures of about 250 °C. Table 2 also lists three new examples of the cation−anion complexes, [Cp*$_2$Yb(bipy-X)][Cp*$_2$YbI$_2$] (X = CO_2Et, OMe, Me), which were isolated from the reaction of the neutral complexes with AgI in toluene, eq 2.

$$Cp^*_2Yb(bipy^-X) + AgI \longrightarrow \text{"}\{[Cp^*_2Yb(bipy\text{-}X)][I]\}\text{"} + Ag$$
$$\downarrow$$
$$1/2\ [Cp^*_2Yb(bipy^-X)][Cp^*_2YbI_2] + 1/2\ bipy\text{-}X \qquad (2)$$

The synthetic reaction yields the desired cation [Cp*$_2$Yb(bipy-H)][I],[1] when the unsubstituted bipyridine is used, which is the reason it is suggested to be an intermediate in eq 2, but the ytterbocene cation−anion pair is isolated when the 4,4′-substituted bipy ligands are used. The reason for the difference is not obvious, but the ion pairs are valuable for their magnetic properties, which is the reason for preparing them.

Infrared spectra in the 300 cm^{-1} region of decamethylytterbocene complexes are a qualitative indicator of the ytterbium oxidation state.[5] An absorption in the range 315−290 cm^{-1} is indicative of Yb(III), whereas an absorption in the range 275−265 cm^{-1} is indicative of Yb(II). This general pattern is apparent for most of the complexes listed in Table 2; two exceptions are the bipy−X derivatives, where X = Me and OMe. These two complexes have low magnetic moments, and the oxidation state

Table 2. Solid State Properties of Ytterbocene Bipyridyl Complexes

compound	color	mp/°C	IR/cm^{-1}	μ_{eff}(300 K)/μ_B
$(Me_5C_5)_2Yb$(bipy-H)[a]	red-brown	328−330	290, 942, 1553	2.4
$(Me_5C_5)_2Yb$(bipy-Me)[a,b]	deep red	>300	271, 944, 1595	0.9
$(Me_5C_5)_2Yb$(bipy-OMe)[b]	deep red	206−208	260, 1602	1.1
$(Me_5C_5)_2Yb$(bipy-Ph)[b]	deep red	245−248	310, 960, 1560	3.3
$(Me_5C_5)_2Yb$(bipy-t-Bu)[b]	red-brown	247−250	310, 1590	2.7
$(Me_5C_5)_2Yb$(bipy-CO_2Et)[b]	red	>330	311, 963, 1534	3.2
$(Me_5C_5)_2Yb$(bipy-CO_2Me)[b]	red	180−181	315, 960, 1540	3.2
$[(Me_5C_5)_2Yb(bipy\text{-}H)]^+[I]^-$ [a]	red-brown	125−130	320, 1598	4.2
$[(Me_5C_5)_2Yb(bipy\text{-}H)]^+[(Me_5C_5)_2YbCl_2]^-$ [a]	red	264−266	1598	6.4
$[(Me_5C_5)_2Yb(bipy\text{-}Me)]^+[(Me_5C_5)_2YbI_2]^-$ [b]	dark red	230	300, 322, 1615	6.2
$[(Me_5C_5)_2Yb(bipy\text{-}OMe)]^+[(Me_5C_5)_2YbI_2]^-$ [b]	dark red	234−235	300, 325, 1610	6.3
$[(Me_5C_5)_2Yb(bipy\text{-}CO_2Et)]^+[(Me_5C_5)_2YbI_2]^-$ [b]	dark red	>320	300, 330, 1550	6.3
$(Me_5C_5)_2Yb(py)_2$[a,c]	dark green	208−210	265	0
$(Me_5C_5)_2Yb(4\text{-picoline})_2$[b]	dark green	228−238	260	0
$(Me_5C_5)_2Yb(py\text{-}OMe)_2$[b]	dark blue	209−211	253	0

[a] From ref 1. [b] This work. [c] From ref 11.

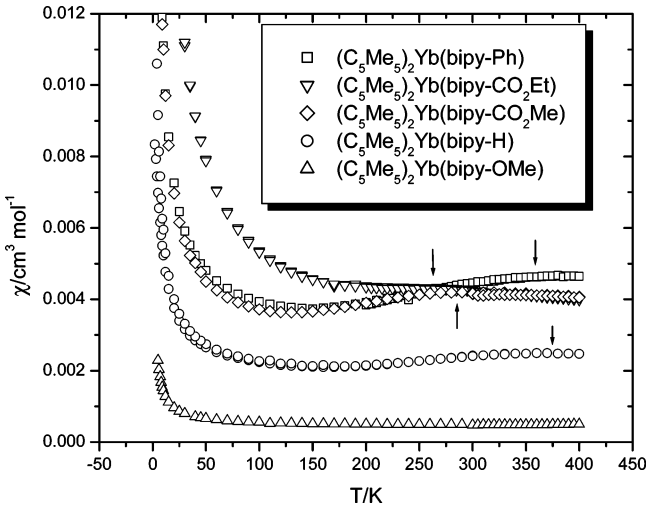

Figure 1. Solid state magnetic susceptibility (χ) vs T plot for $(C_5Me_5)_2$Yb(bipy-Ph), $(C_5Me_5)_2$Yb(bipy-CO_2Et), $(C_5Me_5)_2$Yb(bipy-CO_2Me), $(C_5Me_5)_2$Yb(bipy-H), and $(C_5Me_5)_2$Yb(bipy-OMe). The arrows indicate the maximum value of χ, χ_{max}. The Curie-tails at low temperature indicate small contributions of Yb(III) impurities, except for $(C_5Me_5)_2$Yb(bipy-CO_2Et), in which χ_{max} is washed out by the impurity, yielding a plateau instead of a maximum. This complex is the most difficult one to crystallize, since it is very soluble in pentane, and therefore the most difficult to purify, although it is obtained in analytically pure form.

of the ytterbium in these complexes, and in several of the other ones, is ambiguous (see later).

Solid State Magnetic Measurements: SQUID. Figure 1 shows the χ vs T plot, and Figure 2 shows the plot of μ_{eff} vs T for four of the substituted bipy−ytterbocene complexes, X = OMe, Ph, CO_2Me, and CO_2Et, along with those of the unsubstituted parent, X = H. The plots for the parent complex are included for calibration purposes using the values published.[1,2] The curves in Figures 1 and 2 define a family of curves in which χ passes through a minimum value then gradually increases through a maximum value as T increases; the χ_{max} value is indicated by the arrow in Figure 1. The values of χ and μ_{eff} depend in a regular way on X, viz., at 400 K, OMe < H < CO_2R (R = Me, Et) ≤ Ph. It is clear that the extent of the paramagnetic condition increases when X = H is replaced by an electron-withdrawing group and decreases when X is an electron-donating group, i.e., with the difference in reduction potential of the bipyridines listed in Table 1. This implies that the exchange coupling increases as the energy of the LUMO increases and, conversely, decreases as the LUMO energy decreases. This in turn implies that as the frontier orbital energy of the substituted bipyridine radical anion is closer in energy to that of the frontier orbital energy of the ytterbocene fragment, the exchange integral increases and the extent of the paramagnetic condition decreases.

The low values for Cp^*_2Yb(bipy-OMe) are not due to random paramagnetic impurities in an otherwise diamagnetic compound. This supposition is shown by the data in Figure 3, which shows the experimentally determined values of χ, corrected for a small amount of a $J = 7/2$ impurity, Yb(III), as outlined in ref 2. Subtraction yields a $\chi_{corrected}$ curve that is essentially independent of temperature, no longer has the "Curie tail", and yields χ values > 0, i.e., a paramagnetic molecule.

The magnetization curves for the bipy−Me complex shown in Figures 4 and 5 are similar at low temperature (T < 205 K) and high temperature (T > 212 K) to those presented in Figures 1 and 3, but they show a dramatic deviation in the temperature range 205−212 K.[12]

In this experiment the sample is cooled rapidly from 300 to 2 K, then slowly heated as data collection commences. The value of χ smoothly decreases with increasing temperature to 205 K, when an abrupt decrease occurs in which χ decreases by 25% from 205 to 212 K. After this abrupt change, χ then decreases smoothly to 300 K, whereupon it gradually increases as the temperature increases to 400 K (Figure 4). On cooling slowly from 400 K, the original curve is retraced until the temperature reaches 212 K, when χ slowly increases as the temperature reaches 200 K. At 200 K, χ abruptly increases over the temperature range 200−192 K, then the original curve is retraced. This hysteresis behavior is reproducible over several cycles of temperature, from sample to sample, and is independent of the applied magnetic field strength (5, 20, 40, and 70 kG). The hysteresis is a solid state property of the molecule Cp^*_2Yb(bipy-Me), which is ascribed to a first-order crystallographic phase transition, as described in the next section.

The magnetization data of the only other alkyl-substituted bipyridine complex, Cp^*_2Yb(bipy-*t*-Bu), is also different from those shown in Figures 1 and 4 and rather more complex (Figure 6). Initial cooling of the sample to 2 K followed by slow heating while collecting the χ-values shows that their values reach a maximum value at $T(1) = 345$ K, but between 355 and 365 K

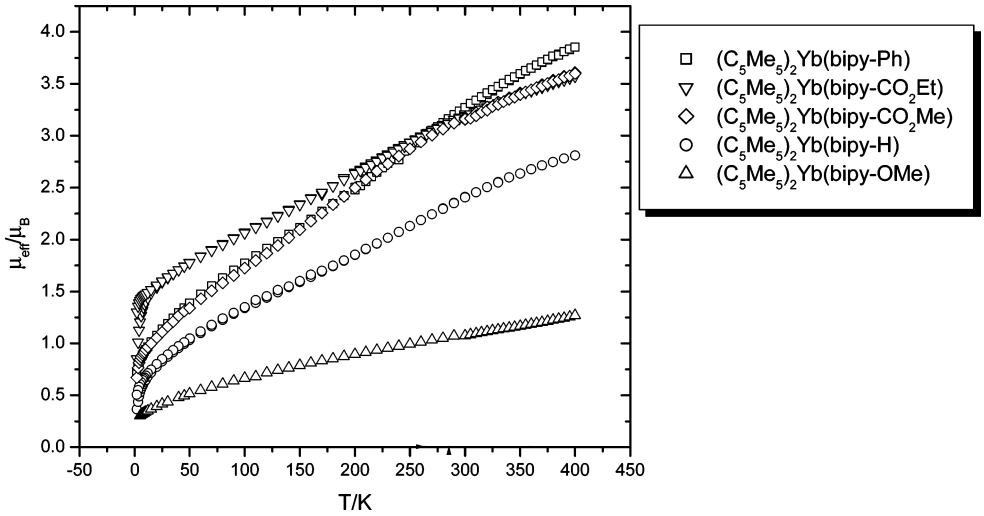

Figure 2. Solid state magnetic moment (μ_{eff}) vs T plot for $(C_5Me_5)_2$Yb(bipy-Ph), $(C_5Me_5)_2$Yb(bipy-CO_2Et), $(C_5Me_5)_2$Yb(bipy-CO_2Me), $(C_5Me_5)_2$Yb(bipy-H), and $(C_5Me_5)_2$Yb(bipy-OMe).

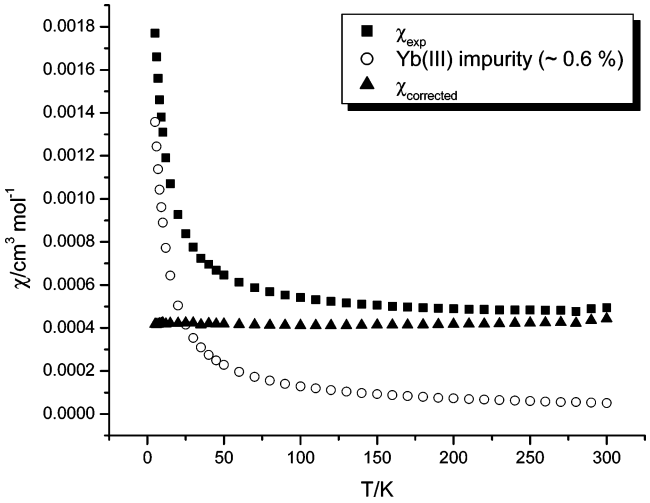

Figure 3. Solid state magnetic susceptibility (χ) vs T plot for $(C_5Me_5)_2$Yb(bipy-OMe). The experimental values χ_{exp} include a small magnetic impurity (~0.6% of a $J = 7/2$ impurity), which is removed in $\chi_{corrected}$. The data clearly show TIP behavior with $\chi_0 = (4.19 \pm 0.05) \times 10^{-4}$ cm^3 mol^{-1}.

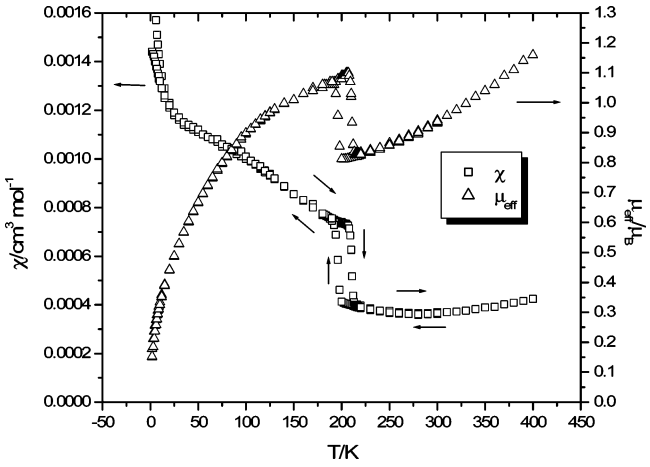

Figure 4. Solid state magnetic susceptibility (χ) vs T plot and magnetic moment (μ_{eff}) vs T plot for $(C_5Me_5)_2$Yb(bipy-Me). The sample was cooled to 2 K, and the data were collected at different fields (5, 20, 40, 70 kG) on heating and cooling cycles.

an abrupt, 50%, drop occurs. On cooling, the original curve is not retraced until the temperature reaches 25 K. Heating slowly does not retrace the initial heating curve, $T(2)$, but path $T(3)$ is followed. The complicated behavior is reproducible and is consistent with the notion that the molecules in the ensemble undergo substantial reorganization and reconstruction, and these changes effect χ.

X-ray Crystallography. An ORTEP diagram of Cp*$_2$Yb(bipy-Me) is shown in Figure 7. Acquisition of the X-ray diffraction data presented several difficulties, since the crystals shatter when placed on a goniometer head that is precooled to 163 K in a stream of liquid nitrogen, the usual way data are collected. In this case, to get diffraction data, the crystal was mounted on a goniometer in a stream of liquid nitrogen cooled to about 225 K and data were collected at 228(2) K, i.e., above the "magnetic hysteresis temperature". The crystallographic data collected at 228(2) K are shown in Table 3, along with those for Cp*$_2$Yb(bipy-H),[1] and bond distances and angles are compared in Table 4 for Cp*$_2$Yb(bipy-Me) and related ytterbocene bipy complexes.[1]

The average Yb−C distance in the bipy−Me complex is slightly longer than that in the bipy complex, 2.67 vs 2.62 Å,

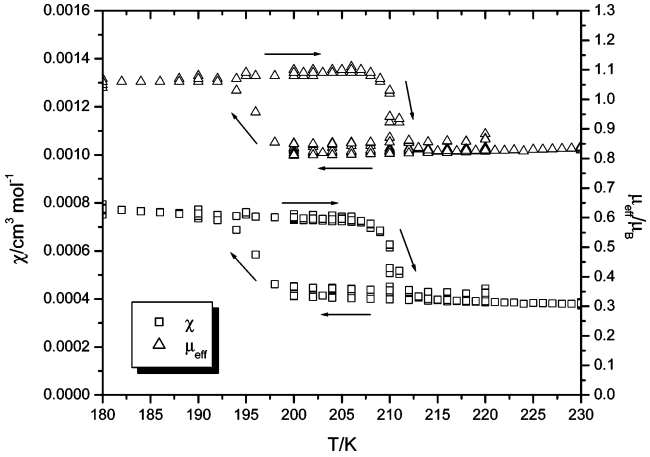

Figure 5. Solid state magnetic susceptibility (χ) vs T plot and magnetic moment (μ_{eff}) vs T plot (180−230 K) for $(C_5Me_5)_2$Yb(bipy-Me). The sample was cooled to 2 K, and the data were collected at different fields (5, 20, 40, 70 kG) on heating and cooling cycles.

as is the Yb−N distance of 2.396(2) and 2.319(6) Å, and the bipy−ring C(2)−C(2′) distance of 1.464(4) and 1.435(9) Å, respectively. The torsion angles are slightly different, with the two rings in the bipy−Me complex being closer to coplanarity. However, these parameters are on the edge of significance and the two molecular structures have nearly identical intramolecular bond distances and angles. After data collection was completed at 228(2) K the temperature of the liquid nitrogen-cooled stream was slowly decreased, and the unit cell parameters were monitored. The unit cell volume decreased smoothly until 185-(2) K (see Supporting Information for the experimental data), whereupon the diffraction pattern changed and the crystal disintegrated to an amorphous powder during the acquisition of the unit cell parameters. Various crystals exhibited identical behavior, although different crystal sizes and cooling rates were explored, resulting in the conclusion that the single crystals undergo a first-order phase transition that irreversibly shatters the crystals in the low-temperature regime that is close to the hysteresis temperature for the polycrystalline material in the magnetic susceptibility study, Figures 4 and 5.

A possible reason for the destructive behavior is traced to the crystal structure of Cp*$_2$Yb(bipy-Me), which crystallizes in the monoclinic crystal system in space group $P2_1/c$, whereas Cp*$_2$Yb(bipy-H) crystallizes in the orthorhombic crystal system in space group *Pbca*.[1] Figures 8 and 9 show the packing diagrams for these two molecules, where the C_5Me_5 rings have been removed for clarity of viewing the intermolecular orientation of the Yb(bipy-X) fragments. The contents of the entire unit cell are available in the Supporting Information. The orthorhombic unit cell for Cp*$_2$Yb(bipy-H), Figure 8, is more open, and the open space follows a zigzag channel that is parallel to the *x*-axis and a cylindrical channel that is parallel to the *z*-axis. Thus, the environment about the individual molecules is open and flexible, so the unit cell will easily accommodate a change in an external variable such as temperature. The unit cell in Figure 8 shows that two Yb(bipy-H) fragments are related by an inversion center located at (0.5, 0, 0), which orientates the bipy ligands so that the carbon atoms in the 3-position of the rings (*meta* carbon atoms) have a C···C distance of only 3.37 Å. This value is close to the interlayer C···C distance of 3.40 Å observed in graphite, from which the van der Waals radius of a carbon atom in an aromatic ring of 1.70 Å is deduced.[13,14] Thus, the C···C distance of 3.37 Å lies very close to the distance at which the repulsive and attractive forces on

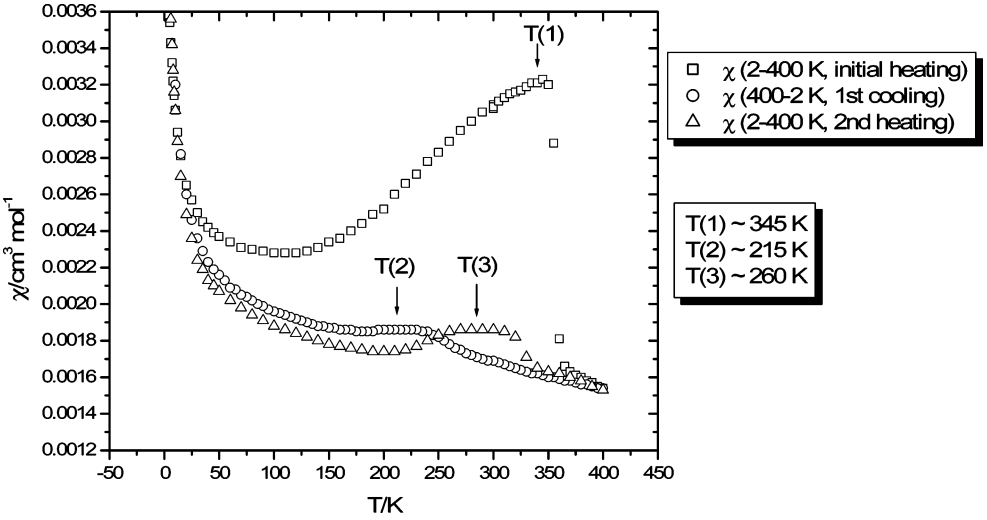

Figure 6. Solid state magnetic susceptibility (χ) vs T plot for $(C_5Me_5)_2Yb(bipy\text{-}t\text{-}Bu)$. The arrows indicate $T(\chi_{max})$, and $T(1)-T(3)$ indicate the different cycles.

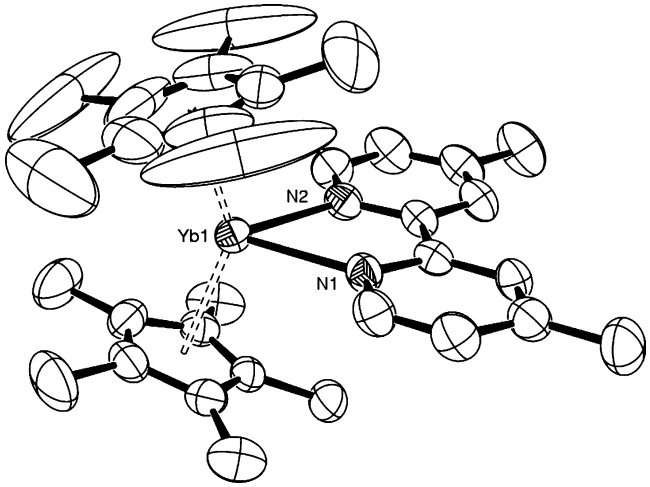

Figure 7. ORTEP diagram of $(C_5Me_5)_2Yb(bipy\text{-}Me)$ (50% probability ellipsoids).

the van der Waals potential energy curve are equal.[15] The monoclinic unit cell for $Cp^*_2Yb(bipy\text{-}Me)$, Figure 9, is less open compared to the orthorhombic unit cell of $Cp^*_2Yb(bipy\text{-}H)$ since the voids are filled with Yb(bipy-Me) fragments and the monoclinic unit cell has fewer degrees of freedom than the orthorhombic one. The individual methyl groups on the 4,4′-position are aligned one on top of the other such that the C−H groups in the 5,5′-positions of the bipyridine ring have C···C contact distances that range from 3.74 to 3.87 Å, with an average distance of 3.82 Å. The C···C distance of 3.82 Å is larger than the closest interplanar distance in $Cp^*_2Yb(bipy\text{-}H)$ and graphite and is close to the distance at which the intermolecular forces of attraction on the van der Waals potential energy curve are at a maximum, 3.8 Å.[15] The intermolecular orientation and interplanar distance of the Yb(bipy-Me) fragments in the unit cell are likely to play an important role in why the crystal shatters on cooling since, as the temperature is reduced from 228 K, the unit cell contracts, forcing all of the molecules in the ensemble closer together. At some temperature the repulsive forces become dominant and the molecules try to find a more open crystalline lattice in order to relieve the lattice pressure. This process is either gradual or sudden; if sudden, the crystal shatters.

The sudden change in the unit cell on cooling is likely to correlate with the hysteresis behavior since the temperature regime at which the crystals shatter and the magnetic hysteresis occurs is comparable. On heating, the molecules in the ensemble expand, but this expansion does not destroy the long-range order. Cooling reconstructs the original order but at a different temperature, which is related to the lattice dynamics in a single crystal relative to that found in a polycrystalline sample. Experiments designed to test this qualitative model are underway.

Table 3. Selected Crystal Data and Data Collection Parameters for $(C_5Me_5)_2Yb(bipy\text{-}H)$ and $(C_5Me_5)_2Yb(bipy\text{-}Me)$

	$(C_5Me_5)_2Yb(bipy\text{-}H)^a$	$(C_5Me_5)_2Yb(bipy\text{-}Me)^b$
formula	$YbN_2C_{30}H_{38}$	$YbN_2C_{32}H_{42}$
fw	599.68	627.72
space group	*Pbca* (#61)	$P2_1/c$
a (Å)	16.976(1)	12.347(1)
b (Å)	30.060(5)	12.907(1)
c (Å)	21.255(3)	18.619(1)
β (deg)	90	104.465(1)
V (Å^3)	10846.4	2873.1(4)
Z	16	4
d_{calc} (g/cm^3)	1.469	1.451
μ(Mo Kα)$_{calc}$ (cm^{-1})	34.56	32.8
size (mm)	0.24 × 0.20 × 0.16	0.22 × 0.20 × 0.12
temperature (K)	298(2)	228(2)
scan type, θ_{max}	$\theta-2\theta$, 22.5°	ω, 24.7°
no. of reflns integrated	7780	12 508
no. of unique reflns, R_{int}	7081, 0.000	4715, 0.0398
no. of good reflns	4494	4088
variables	595	328
transmission range	0.66−0.56	0.69−0.53
R_1	0.033	0.0343
wR_2	0.034	0.0917
R_{all}	0.092	0.0403
GOF	1.653	1.073

[a] Taken from ref 1. [b] This work.

Solution ^{1}H NMR Spectroscopy. The ^{1}H NMR spectra are more sensitive than the infrared and perhaps even the UV−vis spectra as a qualitative determination of whether a molecule is paramagnetic or diamagnetic, particularly when its magnetic moment is low, as is the case for the ytterbocene−bipyridine complexes.[1,2] The proton chemical shifts in a paramagnetic molecule are determined by the Fermi contact, δ^{Fc}, and pseudocontact (dipolar), δ^{pc}, terms, both of which describe the

(15) Devic, T.; Yuan, M.; Adams, J.; Fredrickson, D. C.; Lee, S.; Venkataraman, D. *J. Am. Chem. Soc.* **2005**, *127*, 14616−14627.

Table 4. Selected Bond Distances (Å) and Angles (deg) for [1,3-(Me$_3$C)$_2$C$_5$H$_3$]$_2$Yb(bipy-H), (C$_5$Me$_5$)$_2$Yb(bipy-Me), (C$_5$Me$_5$)$_2$Yb(bipy-H), and [(C$_5$Me$_5$)$_2$Yb(bipy-H)]$^+$[(C$_5$Me$_5$)$_2$YbCl$_2$]$^-$

	[1,3-(Me$_3$C)$_2$C$_5$H$_3$]$_2$Yb(bipy-H)[a]	(C$_5$Me$_5$)$_2$Yb(bipy-Me)[b]	(C$_5$Me$_5$)$_2$Yb(bipy-H)[a]	[(C$_5$Me$_5$)$_2$Yb(bipy-H)]$^+$[(C$_5$Me$_5$)$_2$YbCl$_2$]$^-$[a,c]
Yb−C$_{ring}$ (mean)	2.75	2.67	2.62	2.59
Yb−C$_{ring}$ (range)	2.674(6)−2.803(6)	2.624(5)−2.695(3)	2.592(9)−2.647(7)	2.582(3)−2.614(3)
Yb−centroid	2.47	2.40	2.34	2.30
centroid−Yb−centroid	132	143	139	142
Yb−N	2.50	2.40	2.32	2.37
torsion angle N−C−C−N	15	0.7	3	7
torsion angle C−C−C−C	19	0.2	3	8

[a] From ref 1. [b] This work. [c] The distances and angles of the Cp*$_2$Yb fragment are average values for the individual ytterbocene fragments.

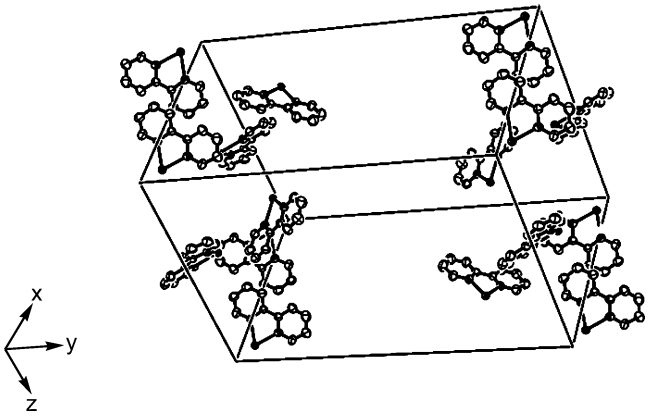

Figure 8. Packing diagram for Cp*$_2$Yb(bipy-H) (50% probability ellipsoids). The Cp* rings have been removed for clarity.

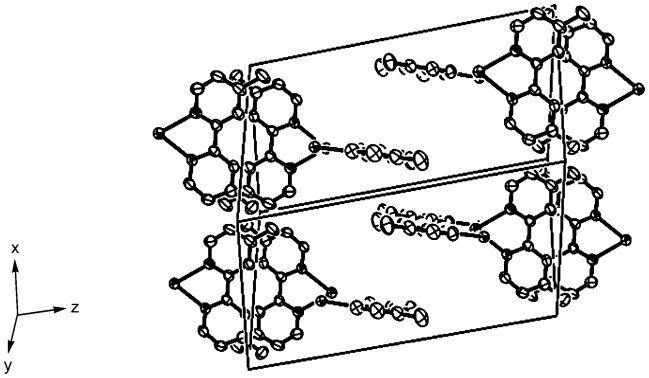

Figure 9. Packing diagram for Cp*$_2$Yb(bipy-Me) (50% probability ellipsoids). The Cp* rings have been removed for clarity.

mechanism by which unpaired spin effects the chemical shift of the ligand and both are proportional to the magnetic susceptibility χ.[16,17] The Fermi contact term is described by eq 3,

$$\delta^{Fc} = -a_i \frac{\gamma_e}{\gamma_H} \frac{g\beta S(S+1)}{3kT} \quad (3)$$

where a_i is the isotropic hyperfine splitting constant. The pseudocontact term, δ^{pc}, for a nonaxially symmetric molecule, depends on through-space interactions of a given nucleus relative to the paramagnetic center as defined in eq 4,

$$\delta^{pc} = -\mathbf{D}\, G(\theta, r)_i - \mathbf{D}'\, G'(\theta, \Omega, r)_i \quad (4)$$

where **D** and **D′** are the magnetic susceptibility tensors and G and G' are the geometric factors, which are related to the distance from the paramagnetic center by r^{-3}. In these molecules in which intermolecular exchange between free and bound bipyridine is slow on the NMR time scale, the resonances whose chemical shifts are determined by δ^{pc} are therefore related to **D** and **D′** and therefore directly proportional to the magnetic susceptibility expressed as χT.[17] This assumes that the chemical shifts in solution are averaged over all molecular orientations and the orientations of the individual molecules are randomly distributed in the polycrystalline powders in the magnetization experiments. The chemically inequivalent bipy resonances should be most sensitive, since they occur over a wide range, but this assumes that they can be assigned. The ^{1}H NMR chemical shifts at 20 °C of the Cp*$_2$Yb(bipy-X) compounds are listed in Table 5. A pattern is reasonably clear since the C$_5$Me$_5$ resonance occurs over a relatively narrow range, 3.3 to 5.5 ppm downfield of Me$_4$Si, and the integrated intensity leaves no doubt about the assignment. The four bipyridine resonances (three in the 4,4′-disubstituted ligands) span a chemical shift range from +215 to −20 ppm, and the chemical shifts of the neutral derivatives follow a pattern. Thus, all seven complexes show a resonance that is strongly deshielded, which is labeled A. Two other resonances, labeled B and C, appear upfield of the A resonances in a rather narrow range of +11 to −20 and +4 to −20, respectively. These A, B, and C resonances are of area ratio 2:2:2. The other resonance(s), labeled D, is (are) easily assigned due its (their) intensity, and their chemical shifts span a relatively narrow range. An assignment of the A, B, and C resonances is possible by noting that the most strongly shifted resonances are likely to be due to those C−H's in closest proximity to the paramagnetic center (whose chemical shifts are determined by the pseudocontact contribution), the A set, and these are assigned to the C−H in the 6,6′-positions of the bipyridine ring (the site *ortho* to the nitrogen atom). The other two resonances, B and C, are then assigned to the hydrogens in either 3,3′- or 5,5′-position (the site *meta* to the nitrogen atom). A choice may be made in Cp*$_2$Yb(bipy-Ph), where the resonance at δ 10.7 is a doublet while the resonance at δ 4.2 is a singlet, and therefore δ 10.7 is located at the 5,5′-site or C and the δ 4.2 resonance is on the 3,3′-site or B. The line width of the resonances in the other complexes is larger than the expected coupling constant and cannot be used to assign them, but the general chemical shift pattern supports the assignment suggested in Table 5.

Assuming these assignments are correct, eqs 3 and 4 show that a plot of the solution chemical shift (at 300 K) of the 6,6′ hydrogens vs χT (at 300 K) in the solid state is linear, Figure 10. As the chemical shift range for the A resonances is relatively large due to the dominance of the pseudocontact term, a better correlation is expected and observed than when the B and C resonances are used. The solid state magnetic susceptibility

(16) Fischer, R. D. Lanthanide and Actinide Complexes. In *NMR of Paramagnetic Molecules*; La Mar, G. N., Horrocks, W. D., Holm, R. H., Eds.; Academic Press: New York, 1973; pp 521−553.

(17) $\chi T = C = \mu_{eff}^2/2.828^2$.

Table 5. ^{1}H NMR Data of Bipyridyl Ytterbocene Complexes[a]

compound	C_5Me_5	bipy−H (A)	bipy−H (B)	bipy−H (C)	bipy−X (D)
$(C_5Me_5)_2$Yb(bipy-H)	3.98 (9)	160.1 (52)	6.4 (48)	−12.9 (14)	H 26.5 (36)
$(C_5Me_5)_2$Yb(bipy-Me)	3.80 (8)	144.1 (60)	8.2 (57)	−9.5 (22)	CH_3 −9.3 (11)
$(C_5Me_5)_2$Yb(bipy-OMe)	4.10 (10)	169.4 (108)	−18.6 (98)	−20.0 (40)	CH_3 1.21 (4)
$(C_5Me_5)_2$Yb(bipy-Ph)	4.21 (10)	178.3 (74)	4.21 (10)	10.7 (15)	*m*,*o*-CH 6.53 (7) *p*-CH −16.8 (10)
$(C_5Me_5)_2$Yb(bipy-*t*-Bu)	3.95 (7)	141.1 (55)	11.4 (45)	−8.9 (10)	*t*-Bu 1.07 (3)
$(C_5Me_5)_2$Yb(bipy-CO_2Me)	4.45 (13)	211.0 (90)	−10.5 (80)	−19.6 (11)	CH_3 4.04 (5)
$(C_5Me_5)_2$Yb(bipy-CO_2Et)	4.43 (18)	209.9 (110)	−9.1 (87)	−19.5 (22)	CH_2 4.66 (41) CH_3 0.82
$[(C_5Me_5)_2$Yb(bipy-H)]I	3.32 (50)	329.0 (410)	57.0 (34)	−15.3 (24)	H 9.2 (30)
$[(C_5Me_5)_2$Yb(bipy-Me)]$^+$	3.61 (72)	330.0 (390)	56.6 (34)	−14.7 (23)	CH_3 8.29 (10)
$[(C_5Me_5)_2YbI_2]^-$	2.76 (32)				
$[(C_5Me_5)_2$Yb(bipy-OMe)]$^+$	5.30 (50)	334.6 (400)	58.4 (34)	−15.3 (24)	CH_3 10.04 (16)
$[(C_5Me_5)_2YbI_2]^-$	4.26 (75)				
$[(C_5Me_5)_2$Yb(bipy-CO_2Et)]$^+$	5.51 (60)	332.9 (500)	58.0 (90)	−13.1 (80)	CH_2 6.50 (60)
$[(C_5Me_5)_2YbI_2]^-$	4.05 (35)				CH_3 3.68 (80)

[a] Recorded in C_6D_6 (neutral complexes) or CD_2Cl_2 (cation−anion complexes) at 20 °C. The line widths at half-peak height (Hz) are given in parentheses.

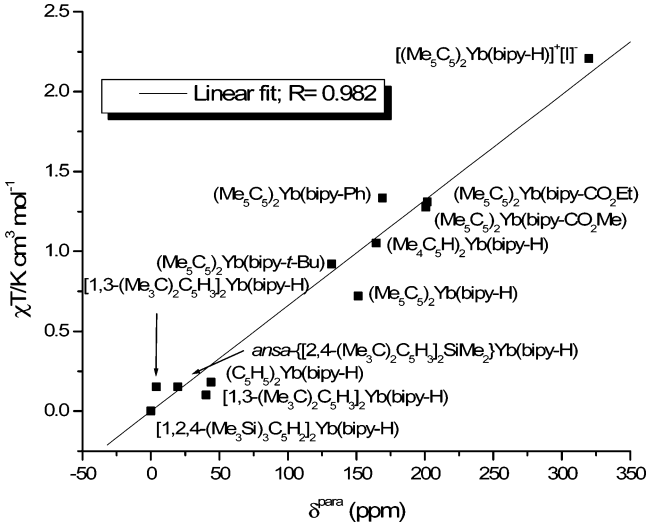

Figure 10. Solid state magnetic susceptibility (χT_{solid}) vs paramagnetic chemical shift (δ^{para}) at 300 K for the "A" set of resonances in various Cp'_2Yb(bipy-X) complexes.

values are used since the solution magnetic moments are likely to have large errors associated with them since the moments are low.[2]

The plot in Figure 10 is anchored by $[1,2,4\text{-}(Me_3Si)_3C_5H_2]_2$Yb(bipy-H), where the 6,6′ resonance is assigned to the most deshielded resonance in the only diamagnetic compound in this series,[1,2] and $[Cp^*_2$Yb(bipy-H)][I], an authentic example of Yb(III), in which the magnetic moment is normal, i.e., without exchange coupling. The assignment of chemical shifts of the bipyridine resonances in the cation and in the cation−anion ion pairs in Table 5 is analogous to that used in the neutral derivatives. Thus the feature identified as A is the most strongly deshielded, on the order of +330 ppm, while the others fall into narrow regions around +57, −15, and +10 ppm due to the B, C, and D resonances. The strong correlation between the isotropic chemical shift, that is, $\delta^{para} = \delta^{obs} - \delta^{dia}$, where δ^{dia} is the chemical shift in $[1,2,4\text{-}(Me_3Si)_3C_5H_2]_2$Yb(bipy-H), of the resonances assigned to the 6,6′-position relative to χT may be extended to the other ytterbocenes described earlier.[1,2] The correlation in Figure 10 supports a thesis developed in this and earlier papers that the magnetic susceptibilities of molecules with low magnetic moments are difficult to measure with confidence and the confidence level increases when two different physical methods correlate, as in Figure 10.

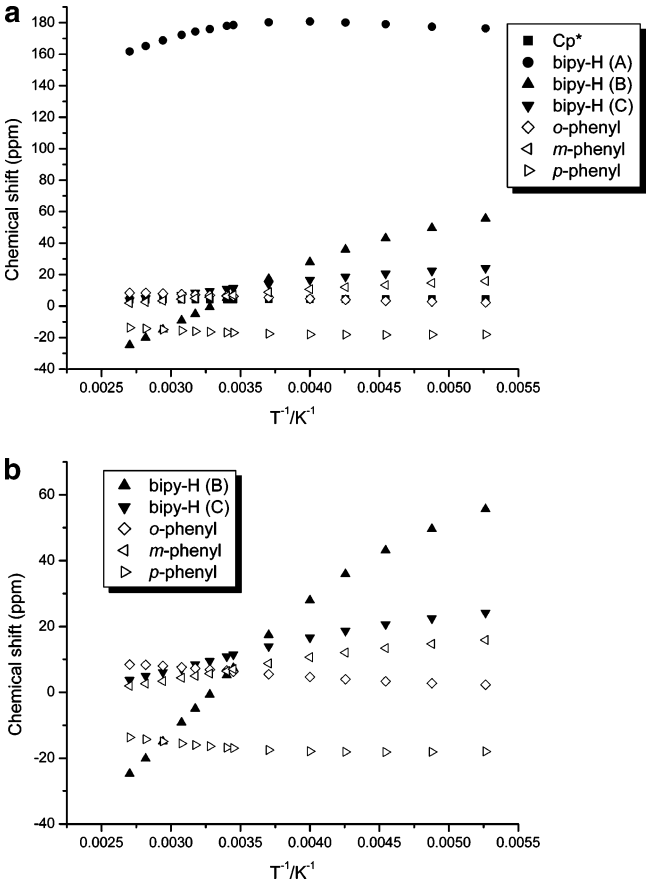

Figure 11. (a) Chemical shift (δ) vs T^{-1} plot of ^{1}H NMR resonances of $(C_5Me_5)_2$Yb(bipy-Ph) in toluene-d_8 at temperatures from −70 to +100 °C. (b) Chemical shift (δ) vs T^{-1} plot of ^{1}H NMR resonances of $(C_5Me_5)_2$Yb(bipy-Ph) in toluene-d_8 at temperatures from −70 to +100 °C. The C_5Me_5 and bipy-H (A) resonances have been omitted for clarity.

The variable-temperature ^{1}H NMR spectra of the decamethylytterbocene complexes with the 4,4′-disubstituted bipyridine are similar to each other and similar to that of Cp^*_2Yb(bipy-H) reported earlier.[1,2] A plot of δ vs T^{-1} for the bipy−Ph derivative is shown in Figures 11a and 11b, and the others are available as Supporting Information. The most deshielded resonance, assigned to A, has a nonlinear temperature dependence, and this pattern is observed in all of the derivatives. The resonance ascribed to B also is nonlinear in T^{-1}, but that due to C has a linear dependence. The nonlinear dependence may

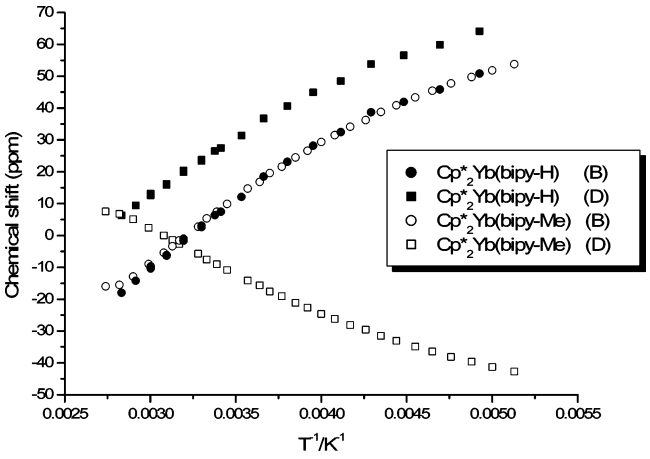

Figure 12. Chemical shift (δ) vs T^{-1} plot of ^{1}H NMR resonances B and D of $(C_5Me_5)_2$Yb(bipy-H) and $(C_5Me_5)_2$Yb(bipy-Me) in toluene-d_8 at temperatures from −70 to +100 °C. The resonances B and D are assigned as 3,3′-H_2-bipy and 4,4′-X_2-bipy (X = H and Me), respectively.

be due to the mechanism by which the unpaired spin density is distributed to the various sites in the molecule, but the separation of the contributions of δ^{pc} and δ^{Fc} is not an easy task except in cubic symmetry, when δ^{pc} vanishes.[18] Experimentally the dominance of the Fermi contact term can be demostrated, since a_H and a_{CH3} have different signs and consequently different slopes as a function of temperature.[19] Thus, when a methyl group replaces a hydrogen atom at a given site in a ligand that is remote from the paramagnetic center, their temperature dependences will have opposite slopes when the Fermi contact shift dominates the pseudocontact shift. The two molecules $(C_5Me_5)_2$Yb(bipy-H) and $(C_5Me_5)_2$Yb(bipy-Me) fit these criteria, and the δ vs T^{-1} plots for the B and D resonances in the two complexes are shown in Figure 12. The B resonances in the two complexes, which are assigned to the C−H's at the 3,3′-site, are superimposable. In contrast the resonances due to the C−H and C−Me groups at the 4,4′-site have opposite slopes. This striking result suggests that the contributions of δ^{pc} and δ^{Fc} to the C−H chemical shifts located in the 3,3′-site are similar but that the δ^{Fc} term dominates the δ^{pc} term for the 4,4′-site. Two additional observations are consistent with this deduction. The temperature dependence of the *tert*-butyl chemical shift in $(C_5Me_5)_2$Yb(bipy-*t*-Bu) (see Supporting Information for details) is essentially independent of temperature, which is consistent with the view that the CMe_3 group is less capable of hyperconjugation than a CH_3 group. In addition, the phenyl ring hydrogens in $(C_5Me_5)_2$Yb(bipy-Ph) in the *ortho* and *para* C−H sites are shielded relative to the chemical shifts in the free ligand. The temperature dependence of the *ortho* and *para* chemical shifts is nonlinear with negative slopes, implying a dominance of the contact term, Figure 11b. The slope of the *meta* C−H is positive and the shift is linear in T^{-1}. Resonance structures are useful to illustrate how negative spin density localizes on the *ortho* and *para* sites. The nonzero contribution of the contact term to the ^{1}H NMR chemical shifts means that unpaired spin density is located in the bipy ring in the ytterbocene complexes.

The nonlinear behavior of the chemical shifts as a function of temperature of the bipy resonances is difficult to rationalize, but it is clear that the shifts are due to intramolecular processes since no exchange between free and bound bipy resonances is observed on the NMR time scale. The nonlinear chemical shifts presumably reflect the change in unpaired spin density at a given site, which is related to the mechanism of transmission of the spin density. Experimental and calculational studies on the mechanism are underway.[3]

Conclusions

This and earlier papers[1,2] show that the 1:1 coordination complexes between ytterbocenes and bipyridine do not have a closed shell electronic configuration, as anticipated from their stoichiometry. The complexes are paramagnetic, and the extent of their paramagnetism, measured by χ or μ_{eff}, depends on the substituents on cyclopentadienyl and bipyridine ligands. In all cases studied, the observed values of χ (or μ_{eff}) are lower than expected for the two uncoupled spin carriers in the molecules represented by the valence bond structure [Yb(III), $4f^{13}$)][bipy$^{\bullet-}$, $S = 1/2$]. The Yb(III) spin carrier is a bent sandwich fragment in which the unpaired electron is located in a b_1-symmetry orbital of f-parentage[20,21] and, therefore, a hole with b_1 symmetry (in molecular C_{2v} symmetry). In addition, an empty b_1-symmetry orbital of d-parentage is available, which is Yb−Cp ring antibonding, that can hybridize with the f-parentage orbitals of the same symmetry. Since the unpaired electron in bipy resides in an orbital with b_1 symmetry (in C_{2v} molecular symmetry),[22] these electrons in the spin carriers can mix, providing a pathway for antiferromagnetic exchange coupling. However, the magnetic susceptibility curves do not fit to a Boltzmann distribution of the two spin isomers with $S = 0$ and $S = 1$, as is the case for Cp_2Ti(bipy);[23] thus the ytterbocene−bipyridine complexes cannot be described by a spin equilibrium model. The Yb L_{III} edge XANES data of Cp*$_2$Yb(bipy) unequivocally show that the ground state is not a single configuration ground state (e.g., it cannot be described by a single wave function), but it is a multiconfigurational or mixed-valent ground state.[3] Thus the mechanism of electron communication in these 1:1 complexes is not trivial to understand using the physical methods familiar to chemists. Further studies using the physical methods available to the physics community will be published when complete.

Experimental Section

General Comments. All reactions and product manipulations have been carried out under a dry nitrogen atmosphere using standard Schlenk and glovebox techniques. Dry, oxygen-free solvents were employed throughout. NMR spectra were taken on Bruker AVQ-400 and AV-300 spectrometers. All chemical shifts are reported in δ units with reference to the residual protons of the deuterated solvents, which are internal standards, for proton chemical shifts. Melting points were measured on a Thomas-Hoover melting point apparatus in sealed capillaries and are uncorrected. The elemental analyses were performed by the analytical facilities at the University of California at Berkeley. Magnetic susceptibility data were obtained on a Quantum Design MPMS XL7 SQUID magnetometer as described previously.[2] $(C_5Me_5)_2$Yb(bipy-Me)[1] and

(18) Bleaney, B. *J. Magn. Reson.* **1972**, *8*, 91−100.
(19) (a) La Mar, G. N.; Horrocks, W. D.; Holm, R. H. *NMR of Paramagnetic Molecules*; Academic Press: New York, 1973; pp 85−178. (b) Wicholas, M.; Drago, R. S. *J. Am. Chem. Soc.* **1968**, *90*, 6946−6950. (c) Horrocks, W. D.; Taylor, R. C.; LaMar, G. N. *J. Am. Chem. Soc.* **1964**, *86*, 3031−3038. LaLancette, E. A.; Eaton, D. R.; Benson, R. E.; Phillips, W. D. *J. Am. Chem. Soc.* **1962**, *84*, 3968−3970.
(20) Green, J. C.; Hohl, D.; Rösch, N. *Organometallics* **1987**, *6*, 712−720.
(21) Ortiz, J. V.; Hoffmann, R. *Inorg. Chem.* **1985**, *24*, 2095−2104.
(22) Kaim, W. *J. Am. Chem. Soc.* **1982**, *104*, 3833−3837
(23) McPherson, A. M.; Fieselmann, B. F.; Lichtenberger, D. L.; McPherson, G. L.; Stucky, G. D. *J. Am. Chem. Soc.* **1979**, *101*, (13), 3425−3430.

$(C_5Me_5)_2Yb(OEt_2)$[11] were prepared as previously reported. The 4,4′-disubstituted 2,2′-bipyridine ligands were purified by crystallization and/or sublimation; 4-picoline and 4-methoxypyridine were distilled from sodium prior to use.

$(C_5Me_5)_2Yb$(bipy-OMe). $(C_5Me_5)_2Yb(OEt_2)$ (0.57 g, 1.1 mmol) and the 4,4′-dimethoxy-2,2′-bipyridine (0.22 g, 1.0 mmol) were weighed into a Schlenk flask and dissolved in 30 mL of toluene with stirring. The dark red solution was stirred for 1 h at room temperature and filtered, and the filtrate was concentrated to ca. 20 mL. Cooling at −20 °C for several days produced large deep red crystals (0.44 g, 0.67 mmol, 67%). Mp: 206−208 °C (rev). Anal. Calcd for $C_{32}H_{42}N_2O_2Yb$: C, 58.26; H, 6.42; N, 4.25. Found: C, 58.24; H, 6.38; N, 4.20. ^{1}H NMR (C_6D_6, 20 °C): δ 169.4 (2H, $\nu_{1/2}$ = 108 Hz, bipy-H), 4.1 (30H, $\nu_{1/2}$ = 9.8 Hz, C_5Me_5), 1.21 (6H, $\nu_{1/2}$ = 3.6 Hz, bipy-OMe), −18.6 (2H, $\nu_{1/2}$ = 98 Hz, bipy-H), −20.0 (2H, $\nu_{1/2}$ = 40 Hz, bipy-H). IR (Nujol mull; CsI windows; cm^{-1}): 2720 (w), 1602 (vs), 1560 (m), 1492 (s), 1422 (s), 1368 (m), 1330 (w), 1310 (m), 1282 (w), 1265 (s), 1248 (m), 1210 (s), 1190 (w), 1102 (w), 1060 (m), 1038 (s), 872 (w), 862 (w), 858 (m), 842 (w), 832 (w), 800 (w), 745 (m), 722 (m), 590 (m), 260 (br s).

$(C_5Me_5)_2Yb$(bipy-Ph). $(C_5Me_5)_2Yb(OEt_2)$ (0.19 g, 0.36 mmol) and the 4,4′-diphenyl-2,2′-bipyridine (0.11 g, 0.36 mmol) were weighed into a Schlenk flask and dissolved in 20 mL of toluene with stirring. The red-purple solution was stirred for 1 h at room temperature, then the solvent was removed under dynamic vacuum, leaving a red-purple powder. The red-purple residue was dissolved in 50 mL of pentane and filtered, and the filtrate was concentrated to ca. 20 mL. Cooling at −20 °C overnight produced deep red crystals (0.1 g, 0.13 mmol, 37%). Mp: 245−248 °C (dec). Anal. Calcd for $C_{42}H_{46}N_2Yb$: C, 67.09; H, 6.17; N, 3.73. Found: C, 66.73; H, 6.36; N, 3.60. ^{1}H NMR (C_6D_6, 20 °C): δ 178.3 (2H, $\nu_{1/2}$ = 74 Hz, bipy-H), 10.7 (2H, $\nu_{1/2}$ = 15 Hz, bipy-H), 6.53 (8H, $\nu_{1/2}$ ≈ 7 Hz, br signal with some coupling structure (overlapping triplet/doublet), *m*,*o*-C_6H_5), 4.21 (32H, $\nu_{1/2}$ = 10 Hz, C_5Me_5 and bipy-H), −16.8 (2H, $\nu_{1/2}$ = 6 Hz, *p*-C_6H_5). ^{1}H NMR (C_7D_8, 21 °C): 178.0 (2H, $\nu_{1/2}$ = 97 Hz, bipy-H), 10.9 (2H, d, $^3J_{CH}$ = 6.4 Hz, bipy-H5,5′), 6.67 (4H, d, $^3J_{CH}$ = 7.2 Hz, *o*-C_6H_5), 6.47 (4H, "t", $^3J_{CH}$ = 6.6 Hz, *m*-C_6H_5), 5.17 (2H, $\nu_{1/2}$ = 50 Hz, bipy-H), 4.22 (30H, $\nu_{1/2}$ = 10 Hz, C_5Me_5), −16.8 (2H, $\nu_{1/2}$ = 10 Hz, *p*-C_6H_5). IR (Nujol mull; CsI windows; cm^{-1}): 1598 (m), 1580 (m), 1560 (br s), 1495 (w), 1488 (w), 1300 (vw), 1290 (m), 1262 (m), 1242 (vw), 1100 (br m), 1022 (m), 1000 (vw), 960 (br m), 880 (w), 800 (br m), 750 (s), 720 (m), 690 (br m), 630 (m), 530 (w), 310 (br s).

$(C_5Me_5)_2Yb$(bipy-*t*-Bu). $(C_5Me_5)_2Yb(OEt_2)$ (0.80 g, 1.6 mmol) and the 4,4′-di(*tert*-butyl)-2,2′-bipyridine (0.43 g, 1.6 mmol) were weighed into a Schlenk flask and dissolved in 20 mL of toluene with stirring. The color changed immediately to dark red-brown. The solvent was removed under dynamic vacuum. The residue was extracted into pentane (30 mL), filtered, concentrated, and cooled to −25 °C overnight, yielding red-brown crystals (0.76 g, 1.07 mmol, 67%). Mp: 247−250 °C (dec). Anal. Calcd for $C_{38}H_{54}N_2Yb$: C, 64.11; H, 7.65; N, 3.94. Found: C, 64.48; H, 7.96; N, 3.75. ^{1}H NMR (C_6D_6, 20 °C): δ 141.1 (2H, $\nu_{1/2}$ = 55 Hz, bipy-H), 11.4 (2H, $\nu_{1/2}$ = 45 Hz, bipy-H), 3.95 (30H, $\nu_{1/2}$ = 7 Hz, C_5Me_5), 1.07 (18H, $\nu_{1/2}$ = 3 Hz, bipy-CMe_3), −8.9 (2H, $\nu_{1/2}$ = 10 Hz, bipy-H). IR (Nujol mull; CsI windows; cm^{-1}): 1610 (m), 1592 (sh m), 1588 (m), 1550 (m), 1405 (m), 1380 (s), 1310 (br w), 1260 (s), 1200 (w), 1198 (vbr vs), 1020 (vbr vs.), 902 (vw), 845 (m), 800 (br vs), 730 (br w), 670 (w), 602 (m), 400 (vbr s), 310 (vbr s), 280 (vbr s).

$(C_5Me_5)_2Yb$(bipy-CO_2Et). 4,4′-Dicarboxylate-2,2′-bipyridine diethyl diester was prepared by esterification of the diacid according to a literature procedure.[24] The crude diester was recrystallized twice from boiling ethanol and then sublimed in an oil pump vacuum at 200 °C. $(C_5Me_5)_2Yb(OEt_2)$ (0.63 g, 1.2 mmol) and the 4,4′-dicarboxylate-2,2′-bipyridine diethyl diester (0.36 g, 1.2 mmol) were weighed into a Schlenk flask and dissolved in 60 mL of pentane with stirring. The orange-red solution was stirred 1 h at room temperature and filtered, and the filtrate was concentrated to 5 mL. Cooling at −80 °C for several days produced deep red crystals (0.79 g, 0.95 mmol, 79%), which collapsed to a brick red powder on exposure to vacuum. Mp: >330 °C (dec). Anal. Calcd for $C_{36}H_{46}N_2O_4Yb$: C, 58.13; H, 6.23; N, 3.77. Found: C, 57.77; H, 6.19; N, 3.75. ^{1}H NMR (C_6D_6, 20 °C): δ 209.9 (2H, $\nu_{1/2}$ = 110 Hz, bipy-H), 4.66 (4H, $\nu_{1/2}$ = 41 Hz, CH_2), 4.43 (30H, $\nu_{1/2}$ = 18 Hz, C_5Me_5), 0.82 (6H, t, $^3J_{CH}$ = 5.2 Hz, CH_3), −9.1 (2H, $\nu_{1/2}$ = 87 Hz, bipy-H), −19.5 (2H, $\nu_{1/2}$ = 22 Hz, bipy-H). IR (Nujol mull; CsI windows; cm^{-1}): 2730 (w), 2626 (w), 2540 (w), 1732 (m), 1708 (vs), 1611 (m), 1534 (vs), 1502 (vs), 1372 (s), 1365 (m), 1284 (s), 1267 (vs), 1202 (vs), 1161 (w), 1134 (sh m), 1116 (s), 1037 (s), 963 (vs), 920 (vw), 862 (br m−s), 800 (br vs), 748 (m−s), 724 (w), 686 (br m), 663 (w), 536 (w), 443 (s), 390 (br s), 311 (s), 294 (w).

$(C_5Me_5)_2Yb$(bipy-CO_2Me). $(C_5Me_5)_2Yb(OEt_2)$ (0.42 g, 0.81 mmol) and the 4,4′-dicarboxylate-2,2′-bipyridine dimethyl diester[25] (0.22 g, 0.81 mmol) were weighed into a Schlenk flask and dissolved in 40 mL of toluene with stirring. The dark red solution was stirred 1 h at room temperature, and the solvent was removed under dynamic vacuum, leaving a red powder. The red residue was dissolved in 100 mL of pentane and filtered, and the filtrate was concentrated to ca. 20 mL. Cooling at −20 °C overnight produced deep red blocklike crystals (0.50 g, 0.70 mmol, 86%). Mp: 180−181 °C (dec). Anal. Calcd for $C_{36}H_{46}N_2O_4Yb$: C, 57.05; H, 5.91; N, 3.91. Found: C, 57.35; H, 5.93; N, 3.75. ^{1}H NMR (C_6D_6, 20 °C): δ 211.0 (2H, $\nu_{1/2}$ = 90 Hz, bipy-H), 4.45 (30H, $\nu_{1/2}$ = 13 Hz, C_5Me_5), 4.04 (6H, $\nu_{1/2}$ = 5 Hz, bipy-CO_2Me), −10.5 (2H, $\nu_{1/2}$ = 80 Hz, bipy-H), −19.6 (2H, $\nu_{1/2}$ = 11 Hz, bipy-H). IR (Nujol mull; CsI windows; cm^{-1}): 3100 (vw), 2720 (vw), 2630 (vw), 2540 (vw), 2400 (vw), 2380 (vw), 1720 (s), 1708 (vs), 1695 (vs), 1540 (vs), 1505 (vs), 1450 (s), 1432 (vs), 1338 (m), 1295 (w), 1288 (m), 1258 (m−s), 1240 (m), 1220 (br vs), 1190 (m), 1115 (s), 1095 (m), 1042 (s), 980 (m), 960 (vs), 905 (w), 880 (vw), 830 (w), 805 (m), 775 (vw), 750 (vs), 735 (vw), 690 (m), 410 (vw), 360 (vw), 350 (vw), 315 (vs).

$[(C_5Me_5)_2Yb$(bipy-Me)$]^+[Cp^*_2YbI_2]^-$. Method 1. Bis(pentamethylcyclopentadienyl)ytterbium 4,4′-dimethyl-2,2′-bipyridine (0.3 g, 0.48 mmol) in toluene (15 mL) was contacted with AgI (0.11 g, 0.48 mmol) for 24 h. The solvent was removed under dynamic vacuum, and the residue was washed with pentane (2 × 10 mL). The precipitate was then dissolved in CH_2Cl_2 (10 mL), and the red CH_2Cl_2 solution was filtered from the silver metal formed in the reaction. Pentane (30 mL) was carefully layered onto the CH_2Cl_2 solution, and diffusive mixing at room temperature overnight resulted in dark red crystals (0.2 g, 0.15 mmol, 63%). Mp: 230 °C (dec). Anal. Calcd for $C_{52}H_{72}N_2I_2Yb_2$: C, 47.14; H, 5.48; N, 2.11. Found: C, 47.62; H, 5.16; N, 2.24. ^{1}H NMR (CD_2Cl_2, 20 °C): δ 330.0 (2H, $\nu_{1/2}$ ≈ 390 Hz, bipy-H), 56.6 (2H, $\nu_{1/2}$ = 34 Hz, bipy-H), 8.29 (6H, $\nu_{1/2}$ = 10 Hz, bipy-Me), 3.61 (30H, $\nu_{1/2}$ = 72 Hz, C_5Me_5), 2.76 (30H, $\nu_{1/2}$ = 32 Hz, C_5Me_5), −14.7 (2H, $\nu_{1/2}$ = 23 Hz, bipy-H). IR (Nujol mull; CsI windows; cm^{-1}): 2720 (w), 1615 (s), 1310 (m), 1268 (w), 1245 (w), 1228 (vw), 1022 (s), 920 (br vw), 895 (vw), 850 (m), 830 (m), 805 (br vw), 732 (br s), 698 (w), 560 (m), 530 (m), 480 (w), 438 (w), 390 (vbr w), 322 (vs), 300 (br s).

Method 2. $(C_5Me_5)_2YbI\cdot thf$[1] (0.12 g, 0.17 mmol) and 4,4′-dimethyl-2,2′-bipyridine (0.03 g, 0.17 mmol) were weighed into a Schlenk tube, and toluene (20 mL) was addded. The slurry was stirred at room temperature overnight, the supernatant was discarded, and the residue was washed with pentane (2 × 10 mL) and extracted into dichloromethane (5 mL). Pentane (30 mL) was carefully layered onto the CH_2Cl_2 solution, and diffusive mixing

(24) Elliot, C. M.; Hershenhart, E. J. *J. Am. Chem. Soc.* **1982**, *104*, 7519−7526.

(25) Garelli, N.; Vierling, P. *J. Org. Chem.* **1992**, *57*, 3046−3051.

at room temperature overnight resulted in dark red crystals (0.08 g, 0.06 mmol, 71%). The physical properties were identical to those obtained by method 1.

$[Cp^*_2Yb(bipy\text{-}OMe)]^+[Cp^*_2YbI_2]^-$. Method 1. Bis(pentamethylcyclopentadienyl)ytterbium 4,4′-dimethoxy-2,2′-bipyridine (0.32 g, 0.48 mmol) in toluene (15 mL) was contacted with AgI (0.11 g, 0.48 mmol) for 24 h. The solvent was removed under dynamic vacuum, and the residue was washed with pentane (2 × 10 mL). The precipitate was then dissolved in CH_2Cl_2 (10 mL), and the red CH_2Cl_2 solution was filtered from the silver metal formed in the reaction. Pentane (30 mL) was carefully layered onto the CH_2Cl_2 solution, and diffusive mixing at room temperature overnight resulted in dark red blocks (0.23 g, 0.17 mmol, 71%). Mp: 234−235 °C (dec). Anal. Calcd for $C_{52}H_{72}N_2O_2I_2Yb_2$: C, 46.02; H, 5.35; N, 2.06. Found: C, 47.20; H, 5.10; N, 2.10. ^{1}H NMR (CD_2Cl_2, 20 °C): δ 334.6 (2H, $\nu_{1/2} \approx 400$ Hz, bipy-H), 58.4 (2H, $\nu_{1/2} = 34$ Hz, bipy-H), 10.04 (6H, $\nu_{1/2} = 16$ Hz, bipy-OMe), 5.30 (30H, $\nu_{1/2} = 50$ Hz, C_5Me_5), 4.26 (30H, $\nu_{1/2} = 75$ Hz, C_5Me_5), −15.3 (2H, $\nu_{1/2} = 24$ Hz, bipy-H). IR (Nujol mull; CsI windows; cm^{-1}): 3060 (w), 2720 (w), 1610 (br s), 1562 (m), 1555 (m), 1502 (m), 1495 (m), 1420 (m), 1350 (s), 1328 (m), 1295 (w), 1287 (w), 1272 (m), 1262 (s), 1232 (br m), 1190 (vw), 1042 (s), 1030 (s), 1008 (w), 920 (vw), 895 (vw), 892 (vw), 875 (vw), 860 (vw), 850 (vw), 840 (vw), 730 (br w), 620 (vw), 600 (w), 400 (br m), 325 (vs), 300 (vs).

Method 2. $(C_5Me_5)_2YbI\cdot thf$[1] (0.12 g, 0.17 mmol) and 4,4′-dimethoxy-2,2′-bipyridine (0.036 g, 0.17 mmol) were weighed into a Schlenk tube, and toluene (20 mL) was addded. The slurry was stirred at room temperature overnight, the supernatant was discarded, and the residue was washed with pentane (2 × 10 mL) and extracted into dichloromethane (5 mL). Pentane (30 mL) was carefully layered onto the CH_2Cl_2 solution, and diffusive mixing at room temperature overnight resulted in dark red blocks (0.078 g, 0.057 mmol, 68%). The physical properties were identical to those obtained by method 1.

$[(C_5Me_5)_2Yb(bipy\text{-}CO_2Et)]^+[Cp^*_2YbI_2]^-$. Bis(pentamethylcyclopentadienyl)ytterbium 4,4′-dicarboxylate-2,2′-bipyridine diethyl diester (0.73 g, 0.98 mmol) in toluene (15 mL) was contacted with AgI (0.23 g, 0.98 mmol) for 24 h. The solvent was removed under dynamic vacuum, and the residue was washed with pentane (2 × 10 mL). The precipitate was then dissolved in CH_2Cl_2 (10 mL), and the red CH_2Cl_2 solution was filtered from the silver metal formed in the reaction. Pentane (30 mL) was carefully layered onto the CH_2Cl_2 solution, and diffusive mixing at room temperature overnight resulted in dark red blocks (0.4 g, 0.32 mmol, 65%). Mp > 320 °C (dec). Anal. Calcd for $C_{56}H_{76}N_2O_4I_2Yb_2$: C, 46.67; H, 5.32; N, 1.94. Found: C, 45.54; H, 5.18; N, 2.02. ^{1}H NMR (CD_2Cl_2, 20 °C): δ 332.9 (2H, $\nu_{1/2} \approx 500$ Hz, bipy-H), 58.0 (2H, $\nu_{1/2} = 90$ Hz, bipy-H), 6.50 (4H, $\nu_{1/2} = 60$ Hz, CH_2), 5.51 (30H, $\nu_{1/2} = 60$ Hz, C_5Me_5), 4.05 (30H, $\nu_{1/2} = 35$ Hz, C_5Me_5), 3.68 (6H, $\nu_{1/2} = 80$ Hz, CH_3), −13.1 (2H, $\nu_{1/2} = 80$ Hz, bipy-H). IR (Nujol mull; CsI windows; cm^{-1}): 3080 (vw), 2720 (vw), 1738 (vs), 1730 (sh), 1615 (m), 1550 (m), 1400 (vs), 1300 (s), 1270 (s), 1250 (s), 1235 (m), 1170 (vbr w), 1140 (s), 1120 (vbr w), 1065 (vw), 1020 (vs), 912 (w), 880 (w), 860 (w), 800 (vbr w), 778 (s), 722 (s), 690 (m−s), 672 (vw), 390 (vbr m), 330 (vs), 300 (br s).

$(C_5Me_5)_2Yb(4\text{-picoline})_2\cdot C_7H_8$. 4-Methylypyridine (1 mL, 1.02 mmol) was added with stirring to a green toluene solution of $(C_5Me_5)_2Yb(OEt_2)$ (0.50 g, 0.97 mmol). The solution immediately became deep blue-green. The solvent was removed under dynamic vacuum, and the residue was washed with pentane and dissolved in hot toluene (20 mL). After filtration, the solution was slowly cooled to −25 °C to give dark green crystals (0.58 g, mmol, 83%), which were found by microanalysis and hydrolysis to contain one toluene of crystallization. The compound was insoluble in pentane and only sparely soluble in toluene. Mp: 228−238 °C (dec). Anal. Calcd for $C_{39}H_{52}N_2Yb$: C, 64.89; H, 7.26; N, 3.88. Found: C, 65.25; H, 6.82; N, 4.03. The low solubility of the product prevented the acquisition of an NMR spectrum in C_6D_6. IR (Nujol mull; CsI windows; cm^{-1}): 2720 (w), 1612 (s), 1505 (m), 1495 (m), 1265 (m), 1230 (w), 1215 (m), 1080 (vbr m), 1020 (vbr m), 1010 (m), 812 (vs), 737 (vs), 730 (sh), 700 (s), 670 (w), 540 (w), 505 (s), 475 (m), 260 (br s).

$(C_5Me_5)_2Yb(py\text{-}OMe)_2$. 4-Methoxypyridine (1 mL, 0.88 mmol) was added with stirring to a green toluene solution of $(C_5Me_5)_2Yb(OEt_2)$ (0.40 g, 0.77 mmol). The solution immediately became deep green. The solvent was removed under dynamic vacuum, and the residue was washed with pentane and dissolved in toluene (20 mL). After filtration, the solution was concentrated and cooled to −25 °C to give dark blue crystals (0.33 g, 0.50 mmol, 65%). Mp: 209−211 °C (dec). Anal. Calcd for $C_{32}H_{44}N_2O_2Yb$: C, 58.08; H, 6.70; N, 4.23. Found: C, 57.92; H, 6.79; N, 4.15. ^{1}H NMR (C_6D_6, 20 °C): δ 8.32 (4H, br s, py-H), 6.36 (4H, br s, py-H), 3.01 (6H, s, *p*-OMe), 2.12 (30H, s, C_5Me_5). A spin−spin coupling for the pyridine−CH resonances was not observed, as the resonances were significantly broadend, suggesting exchange on the NMR time scale. IR (Nujol mull; CsI windows; cm^{-1}): 3050 (m), 3030 (m), 2720 (w), 1608 (s), 1568 (m), 1550 (s), 1340 (w), 1302 (vs), 1210 (s), 1040 (vs), 1002 (s), 860 (w), 820 (s), 696 (w), 660 (vw), 572 (w), 550 (w), 470 (w), 375 (br w), 253 (br s).

Crystallographic data are deposited with the Cambridge Crystallographic Data Centre. Copies of the data (CCDC 292029) can be obtained free of charge via http://www.ccdc.cam.ac.uk/data_request/cif, by e-mailing data_request@ccdc.cam.ac.uk, or by contacting The Cambridge Crystallographic Data Centre, 12 Union Road, Cambridge CB 1EZ, UK; fax +44 1223 336033.

Acknowledgment. This work was supported by the Director, Office of Energy Research, Office of Basic Energy Sciences, Chemical Sciences Division of the U.S. Department of Energy under Contract No. DE-AC03-76SF00098. We thank Dr. Fred Hollander and Dr. Allen Oliver for assistance with the crystallography and the German Academic Exchange Service (DAAD) (M.D.W.) and the NSERC (Canada) (D.J.B.) for fellowships. We thank Wayne W. Lukens and Corwin H. Booth for endless hours of discussion about what these molecules are trying to tell us.

Supporting Information Available: Crystallographic data, labeling diagrams, tables giving atomic positions, anisotropic thermal parameters, bond distances, bond angles, torsion angles, least-squares planes, packing diagrams, temperature dependence of the unit cell parameters of $(C_5Me_5)_2Yb(bipy\text{-}Me)$, and variable-temperature ^{1}H studies. This material is available free of charge via the Internet at http://pubs.acs.org. Structure factor tables are available from the authors.

OM051051D